Metabolism of β-Methyl-Heptadecanoic Acid in the Perfused Rat Heart and Liver

Guy D. Fink, Jane A. Montgomery, France David, Michel Garneau, Eli Livni, David Elmaleh, H. William Strauss, and Henri Brunengraber

Departments of Biochemistry and Nutrition, University of Montreal, Montreal, Canada; and the Division of Nuclear Medicine, Massachusetts General Hospital, Boston, Massachusetts

The metabolism of β-methyl-[1-^{14}C]heptadecanoic acid, a potential myocardial imaging agent, was investigated in perfused hearts and livers from rats. Hepatic uptake is ~4.5 times greater than cardiac uptake. In the heart, 66% of β-methyl-heptadecanoic acid metabolism occurs via omega-oxidation, 33% by esterification and <1% via alpha-oxidation. In contrast, 53% of hepatic metabolism of β-methyl-heptadecanoic acid occurs via alpha-oxidation, 27% via omega-oxidation, and 20% via esterification. Perfusion of hearts and livers with concentrations of β-methyl-heptadecanoic acid 100 to 1000 times greater than that used for myocardial imaging does not alter any of the physiological and biochemical parameters measured. In the perfused liver, 3-methyl-[1-^{14}C]glutarate was identified as the principal hydrosoluble catabolite of β-methyl-heptadecanoic acid.

J Nucl Med 1990; 31:1823–1830

Noninvasive imaging of the myocardium yields information on regional blood flow and cardiac metabolism. Flow markers such as thallium-201 (^{201}Tl) have been extensively used for detection of obstructive myocardial disease (*1–3*). Since fatty acids (FA) contribute a sizeable fraction of the fuel used by the heart, iodine-123 (^{123}I) and carbon-11- (^{11}C) labeled FA have also been used for noninvasive cardiac imaging (*4–9*). Carbon-11 labeling of the carboxyl of a FA can be conveniently achieved by reacting an alkyl-magnesium bromide with $^{11}CO_2$ generated in a cyclotron (*6–12*). Because of the rapid metabolism of straight-chain FAs in the myocardium, radioactivity is released from the heart within minutes, preventing precise tomography of the organ. Modified fatty acids (MFA) have been designed to resist oxidation. β-Methyl-heptadecanoic acid (BMHDA) is one of these compounds whose beta-oxidation is blocked at the level of L-3-hydroxyacyl-CoA dehydrogenase (*10–12*). Preventing beta-oxidation increases the residence time of the tracer in the heart up to an hour, thus allowing detailed positron emission tomography (PET). Livni et al. (*10*) demonstrated that after injection of [^{14}C]BMHDA to live rats, the tracer concentrates mostly in heart and liver.

In view of the promising features of BMHDA, we investigated the fate of [1-^{14}C]BMHDA in perfused hearts, livers, and hearts and livers from rats. The concentrations of labeled BMHDA used (0.10 and 0.75 m*M*) are 100 to 1000 times greater than the maximal concentration reached during clinical imaging. We demonstrate that BMHDA is slowly metabolized by a combination of alpha- and omega-oxidation. Further, BMHDA does not have any detectable deleterious effect on rat heart or liver.

EXPERIMENTAL PROCEDURES

Materials

Enzymes, coenzymes, and biochemicals were purchased from Boehringer (Montreal, Canada) and Sigma (St. Louis, Mo.). RS-BMHDA was a generous gift from McNeil Pharmaceuticals. Tri-Sil/BSA was obtained from Pierce Chemical. RS-β-Methyl-[1-^{14}C]heptadecanoic acid and [1-^{14}C]stearic acid were obtained from New England Nuclear (N. Billerica, MA). [1-^{14}C]BMHDA was purified on preparative C-18 HPLC column (MCH-10, 30 cm × 8 mm, Varian) developed first with 1% acetic acid in methanol then with CH_2Cl_2. Radiochemical purity (>99%) was assessed by thin-layer chromatography (TLC) on silica plates (Redi-Coat-2D, Supelco) developed with hexane:diethyl ether:acetic acid (85:15:1). A stock solution of 40 m*M* sodium BMHDA was prepared in 15% bovine serum albumin dissolved in saline (13).

Animals

Male Sprague-Dawley rats (300–400 g; Charles River) were kept in a controlled environment (22°C to 24°C) and fed Charles River rat chow ad libitum. Rats used as liver donors were starved for 48 hr before use. All heart donors received an intraperitoneal injection of 2000 U/Kg heparin 1 hr before surgery.

Heart Perfusions

Hearts were perfused in the working mode (*14–16*) with Krebs-Ringer bicarbonate buffer containing 2% dialyzed bovine serum albumin (fraction V, fatty acid poor, Miles Sci-

Received Oct. 11, 1989; revision accepted April 25, 1990.

For reprints contact: Henri Brunengraber, Research Center, Notre-Dame Hospital, Montreal, QC, H2L 4M1, Canada.

entific (Kanakee, Il), 1.3 m*M* Ca^{++}, 5 m*M* glucose and 5 U/l of crystalline beef and pork insulin. After 15 min equilibration, 0.1 m*M* BMHDA was added, either unlabeled or at a specific activity of 1.0 Ci/mol.

Liver Perfusions

The surgical procedure and perfusion apparatus were as described previously (*17*) except that gas flow was stopped and the oxygenator sealed, just before labeled BMHDA was added to the perfusate (*18*). Livers were perfused with 150 ml Krebs-Ringer bicarbonate buffer containing 4% dialyzed bovine serum albumin (fraction V, fatty acid poor, Miles) and 5 m*M* glucose. The perfusion medium was maintained at pH 7.40 by an automatic titrator (Radiometer) that dispensed 0.3 N NaOH. After 30 min equilibration, either 0.1 or 0.75 m*M* β-methyl-[1-^{14}C]heptadecanoate (0.60 Ci/mol) was added to the perfusate. During some experiments, influent and effluent pO_2 were measured with O_2 electrodes (Radiometer).

Combined Heart and Liver Perfusions

Apparatus of individual systems were combined in parallel with a shared glass-bulb oxygenator and perfusion reservoir. Two animals were used for surgery. The perfused heart was set up first followed by the liver. Total surgical time for preparation of heart and liver was less than 30 min. Modified Krebs-Ringer buffer (250 ml) described for heart perfusions was used for combined perfusions.

Analysis of Perfusate Samples

Triplicate samples of perfusate were taken. One set of samples was deproteinized with $HClO_4$ (final concentration 3% v/v). Glucose, lactate, and pyruvate were assayed enzymatically (*19,20*) in the neutralized extracts. Another set of samples was acidified with acetic acid, gassed for 20 min with N_2 to eliminate $^{14}CO_2$, and counted in ACS (Amersham) for non-volatile radioactivity. A third set of samples was extracted by the method of Folch (*21*) for lipid analysis. This procedure extracted 99% of the BMHDA from the perfusate. All the radioactivity found in the organic phase corresponded to BMHDA (tested by TLC as described below).

Analysis of Tissue Samples

At the end of experiments, organs were freeze-clamped and stored in liquid nitrogen. Frozen tissue was powdered at the temperature of liquid nitrogen. One aliquot of powder was used to determine the dry wt/wet wt ratio. A second aliquot was used to determine concentration of free coenzyme A, short-chain and long-chain acyl-CoA derivatives (*22*). A third aliquot was extracted with 4 volumes of 8% v/v $HClO_4$ in 40% v/v ethanol. The supernatant was neutralized with 2 N KOH + 0.5 N triethanolamine. The neutralized extract was used to determine ATP, ADP, AMP, and creatine phosphate by enzymatic methods (*23–25*). $HClO_4$ precipitate was extracted for lipid analysis with 19 ml/g of $CHCl_3$:MeOH (2:1) as described by Folch (*21*). Five microliters of the Folch-extract was chromatographed on a TLC plate (LK SD, Whatman), which was developed with hexane:diethyl ether:acetic acid (85:15:1). The different classes of lipids were identified by comparison with the migration of standards. Each band was scraped and its radioactivity counted in ACS.

$^{14}CO_2$ Quantitation

The liver perfusion apparatus was tightly sealed after addition of labeled BMHDA. At the end of the experiment, volatile $^{14}CO_2$ and perfusate bicarbonate were trapped by adding 1 ml of 10 N NaOH to the perfusate (*18*). In heart perfusions, effluent gas from the oxygenator and bicarbonate from the final perfusate were recovered separately. $^{14}CO_2$ was evolved from the continuously gassed oxygenator as described previously (*26*), except that the trapping solution was 1 N NaOH, and the counting fluid was Hionic Fluor (Packard).

Determination of β-methyl Dicarboxylic Acids

Final perfusates from heart and liver were assayed for the presence of 3-methyl-dicarboxylic acids by (a) anion exchange chromatography and (b) gas chromatography-mass spectrometry (GC-MS).

Ten milliliters of final perfusate from a liver perfused with 0.75 m*M* [1-^{14}C]BMHDA was used to assay labeled hydrosoluble substrates. After precipitation of proteins with $HClO_4$ and centrifugation, the supernatant was neutralized and diluted fourfold. The solution was loaded onto a column (1.5 × 20 cm) of AG-1-X8 chloride. After rinsing the column for 10 min with water, the chromatogram was developed (3.5 ml/fraction; 1.4 ml/min) with a linear gradient made up of 200 ml H_2O + 200 ml 0.04 N HCl. After 49 fractions, the eluant was sequentially changed to 20 ml of 0.04, 0.1, 0.5, and 1.0 N HCl every 15 min. A 1-ml aliquot of each fraction was counted for radioactivity in ACS.

To identify 3-methyl-dicarboxylic acids, GC-MS analysis was conducted on (a) extracts from 20 to 40 ml of final heart perfusate deproteinized with sulfosalicylic acid, and (b) pools of four fractions from anion exchange chromatography. All samples were saturated with NaCl, acidified with HCl to pH 1, and extracted four times with diethyl ether (*27*). After evaporation of most of the ether, the residue was derivatized with 0.1 milliliter Tri-Sil/BSA and injected (2 μl) into the GC-MS. The injection port of the GC and the transfer line to the MS were kept at 250° and 280°, respectively. A fused silica capillary column (HP-5; 25 m × 0.2 mm) with helium flow 0.7 ml/min was used to separate the TMS derivatives of extracts from the various preparations. Column temperature, initially set at 80°, increased by 8°/min until it reached 250°, and was maintained at this temperature for 2 min. Electron impact mass spectra and selected ion monitoring were carried out at an ionizing energy of 70 eV. Chemical ionization GC-analyses were conducted under similar conditions except that ammonia gas pressure was 1 to 2 × 10^{-4} torr and electron energy, 250 V. Areas under GC-MS peaks were determined by computer integration. Identification and assay of 3-methylglutarate was done by comparison with external standards of authentic 3-methylglutarate.

RESULTS

A number of physiologic and biochemical parameters were monitored before and after the addition of 0.1 m*M* BMHDA to the heart perfusate. These included: heart rate, coronary flow, aortic flow, O_2 consumption, production of lactate and pyruvate, [lactate]/[pyruvate] ratio (Table 1). In heart tissue, parameters monitored were: concentration of ATP, ADP, AMP, creatine phos-

TABLE 1
Accumulation of Lactate Plus Pyruvate and [lactate]/[pyruvate] Ratio from Perfused Working Hearts

	lactate + pyruvate (m*M*)	[lactate]/[pyruvate]
Control		
15 min	0.23 ± 0.03	4.9 ± 0.5
30 min	0.36 ± 0.05	4.8 ± 0.4
+ BMHDA		
15 min	0.22 ± 0.09	5.8 ± 1.1
30 min	0.36 ± 0.02	6.0 ± 1.0

Results are expressed as mean ± s.e. (n = 6). Hearts were perfused with 0.1 m*M* of oleate for control and 0.1 m*M* of BMHDA.

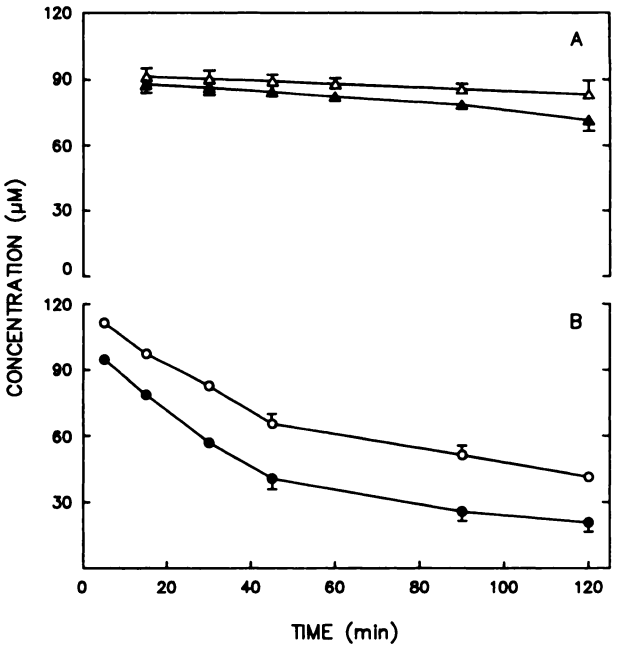

FIGURE 1
Uptake of BMHDA in perfused rat hearts and livers. Hearts (A) and livers (B) were perfused with buffer containing 5 m*M* glucose and 0.1 m*M* [1-^{14}C]BMHDA. Concentrations of BMHDA (▲, ●) and of total non-volatile radioactivity (△, ○) are presented as the mean ± s.e. (n = 5).

phate, free coenzyme A, and short-chain and long-chain acyl-CoA derivatives (Table 2). None of the perfusate or tissue parameters showed any change as a result of BMHDA administration.

In liver perfusions, addition of 0.1 m*M* BMHDA did not affect O_2 consumption. However, addition of 0.75 m*M* BMHDA led to a transient (less than 3 min) 15% increase in O_2 uptake (not shown). In control experiments, addition of 1 m*M* oleate to the perfusate led to a sustained 40% increase in O_2 consumption as reported by others (*28*).

The concentration profiles of BMHDA and of total non-volatile radioactivity (expressed as equivalents of BMHDA) in the perfusate are shown in Figure 1. The heart takes up BMHDA more slowly than the liver. Concentration of BMHDA in the heart perfusate falls by 16 μ*M* in 105 min (panel A) versus 74 μ*M* in 115 min for the liver (panel B). The integrated uptake of BMHDA was 16.1 ± 3.9 (s.e., n = 5) nmol/g × min in the heart, and 8.0 ± 0.8 (n = 6) nmol/g × min in the liver. (The average wet weight of hearts and liver were 1.50 and 11.9 g, respectively.) The profile of the total radioactivity concentration in perfusate parallels that of BMHDA concentration. The difference between the two curves represents hydrosoluble labeled catabolites of BMHDA other than $^{14}CO_2$. The uptake of BMHDA and the total radioactivity were similar for combined perfusions (heart + liver) and liver perfusions during the first 30 min of experiments. Therefore, data from dual perfusions mainly reflect hepatic uptake and catabolism of BMHDA.

Hearts and livers perfused with labeled BMHDA generated $^{14}CO_2$. In the heart, $^{14}CO_2$ production was 0.13 ± 0.02 nmol/min (n = 6), whereas in the liver it was 41.8 ± 5.4 nmol/min (n = 6). When expressed as per gram of tissue, the rates of $^{14}CO_2$ production were nearly 44 times greater in the liver than in the heart.

After 2 hr of perfusion, 4.9% of initial 0.1 m*M* [1-^{14}C]BMHDA had been catabolized via alpha- and omega-oxidation in the heart as compared to 51% in liver (Table 3). The production of $^{14}CO_2$, representing alpha-oxidation, amounted to 0.06% and 33% of the dose of radioactivity in hearts and livers, respectively. Hydrosoluble radioactivity in the perfusate, represent-

TABLE 2
Concentrations of ATP, ADP, AMP, Creatine Phosphate, Free CoA, and Acyl-CoA Derivatives from Perfused Working Hearts

	ATP	ADP	AMP	Creatine phosphate	Free CoA	Short-chain acyl-CoA	Long-chain acyl-CoA
Control	21.7 ± 0.7	5.40 ± 0.28	1.02 ± 0.11	7.2 ± 1.2	0.14 ± 0.03	0.07 ± 0.01*	0.23 ± 0.04
BMHDA	23.9 ± 1.7	6.00 ± 0.21	0.97 ± 0.07	7.0 ± 0.8	0.08 ± 0.02	0.05 ± 0.01	0.20 ± 0.02

Concentrations are expressed as micromoles/g dry weight (mean ± s.e., n = 6). Hearts were perfused with 0.1 m*M* of oleate for control and 0.1 m*M* of BMHDA.

* n = 5 for control of short-chain acyl-CoA.

TABLE 3
Distribution of [1-^{14}C]BMHDA in Lipid Pools from Perfused Liver and Heart

	Heart		Liver	
	30 min	110 min	30 min	110 min
Phospholipids	7.8 ± 0.1	4.6 ± 0.3	27.5 ± 1.3	43.0 ± 2.7
Cholesterol*	2.6 ± 0.2	1.4 ± 0.1	0.9 ± 0.1	0.2 ± 0.1
NEFA	24.5 ± 3.6	11.4 ± 0.8	13.4 ± 1.7	7.7 ± 2.2
Diglycerides	6.9 ± 0.5	5.9 ± 0.5	14.9 ± 1.5	9.6 ± 2.5
Triglycerides	58.9 ± 3.1	76.5 ± 1.3	39.4 ± 3.1	16.5 ± 3.1
Esters of chol.	—	0.4 ± 0.1	3.9 ± 0.5	23.0 ± 2.3

Results are expressed as percentages of total radioactivity of the lipid extract deposited on the TLC (mean ± s.e., n = 5). The 30-min results correspond to combined heart + liver perfusion with the same perfusate. Hearts and livers were perfused with 0.1 m*M* of [1-^{14}C]BMHDA. Lipids were extracted by Folch's method and isolated by TLC (see Materials and Methods).

* Radioactivity found in the cholesterol zone is ascribed to the tail of NEFA migration.

ing omega-oxidation, accounts for 4.3 and 17.4% of the initial radioactivity added in heart and liver perfusions, respectively.

During a 2-hr liver perfusion with 0.75 m*M* [1-^{14}C] BMHDA, concentration of BMHDA fell by 0.44 m*M*. Hydrosoluble radioactivity accumulated to 0.1 m*M*. $^{14}CO_2$ production was 131 nmol/min, representing 14% of the initial radioactivity added.

Triglycerides represent the main form (76.5 ± 1.3%) in which BMHDA is stored in perfused hearts (Table 4). A substantial fraction of radioactivity in heart tissue (11.4 ± 0.8%) was found as nonesterified fatty acids even after 2 hr of perfusion. Analysis of hepatic tissue lipids showed that, after 30 min of perfusion, BMHDA was also stored mainly as triglycerides (39.4 ± 3.1%). Phospholipids accounted for 27.5 ± 1.3% of BMHDA stored. However, after 2 hr of perfusion, the distribution of BMHDA within hepatic lipid pools changed to 43.0 ± 2.7% as phospholipids and 23.0 ± 2.3% as cholesterol esters.

Extracts of heart and liver final perfusates were analyzed by GC-MS to identify some of the catabolites of BMHDA. The gas chromatogram was scanned by mass spectral comparison for the presence of TMS derivatives of 3-methyl-dicarboxylates. No such compounds were identified when concentration of BMHDA in perfusate was 0.1 m*M*. In the perfusate of a liver perfused with 0.75 m*M* BMHDA, we identified 3-methylglutarate, TMS ester with a molecular weight of 290 daltons.

Standard di-TMS-3-methylglutarate elutes at 11.5 min. Its electron impact mass spectrum is shown in Figure 2A. There is no molecular ion at m/z 290 but there are peaks at m/z 117, 147, 172, and 275. The $[M-15]^+$ fragment (m/z 275) is formed by the loss of a methyl group from one of the TMS radicals. Alpha-cleavage results in either the formation of $[TMS\text{-}COO]^+$

TABLE 4
Balance of Radioactivity in Perfusions with [1-^{14}C] BMHDA

	Heart (n = 5)	Liver (n = 6)
Samples withdrawn during perfusion	13.6 ± 0.4	15.8 ± 0.6
Final perfusate:		
Hydrosoluble	4.3 ± 0.5	17.4 ± 1.3
Organosoluble	72.5 ± 2.6	17.0 ± 3.5
$^{14}CO_2$ production	0.06 ± 0.01	33.3 ± 1.8
Tissue composition:		
Hydrosoluble	0.15 ± 0.04	0.20 ± 0.02
Organosoluble	2.9 ± 0.5	12.8 ± 1.1
Percentage of total radioactivity recovered	93.6 ± 3.6	96.1 ± 3.4

Data are presented as percentages of the total radioactivity added at t = 0 to the perfusate (mean ± s.e.). Hearts and livers were perfused with 0.1 m*M* of [1-^{14}C]BMHDA during 110 and 120 min, respectively.

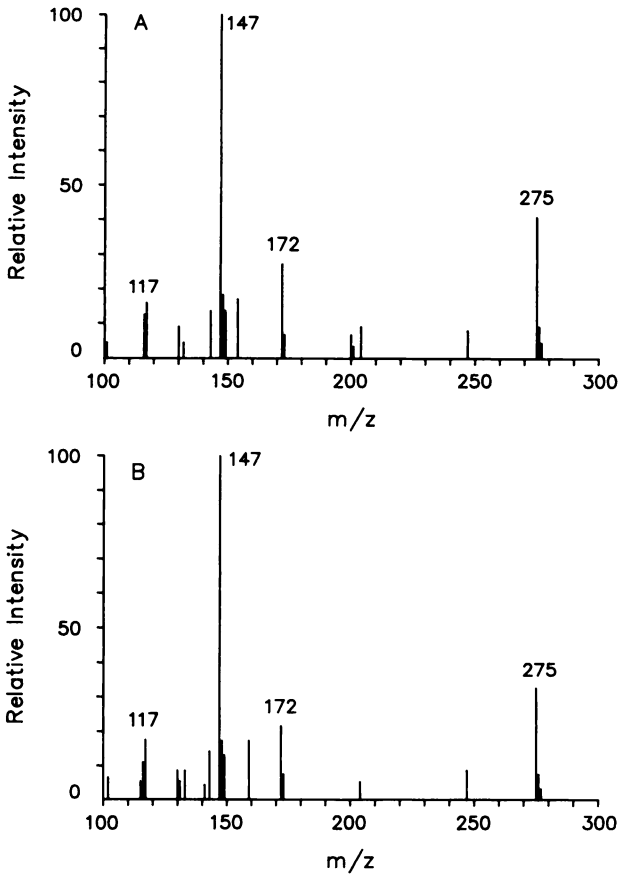

FIGURE 2
Mass spectrum of di-TMS-3-methylglutarate under electron impact ionization. (A) The spectrum of a standard of 3-methylglutarate. (B) The mass spectrum of a rat liver perfusate extract 11.5 min after injection into the GC-MS.

(m/z 117) or $[M-118]^{+\cdot}$ (m/z 172). The latter results from the transfer of a proton to the carboxyl group during fragmentation. The peak at m/z 147 is characteristic of di-TMS compounds, and is, thus, not specific for identification of 3-methylglutarate. To determine 3-methylglutarate concentrations using electron impact, the selected ions monitored are m/z 117, 172, and 275.

Figure 2B shows the corresponding spectrum of 3-methylglutarate in liver perfusate from an experiment using 0.75 m*M* BMHDA. Concentration of 3-methylglutarate, in the final perfusate was 0.04 m*M*, accounting for 25% of the hydrosoluble radioactivity at the end of the experiment.

Confirmation of the identification of 3-methylglutarate was obtained by ammonia chemical ionization (Fig. 3A-B). The $[M + H]^+$ fragment (m/z 291) corresponds to the pseudo-molecular ion. The $[M + NH_4]^+$ ion (m/z 308) results from the addition of ammonia to the parent molecule. The spectra in Figure 3A and 3B show minor peaks which are attributed to noise because of the absence of satellite peaks corresponding to natural abundance of heavy isotopes. Significant amounts of other dicarboxylic acids were not formed in the perfusate.

Figure 4A shows the anion-exchange chromatogram of water soluble radioactivity in perfusate of a liver perfused with 0.75 m*M* [1-^{14}C]BMHDA. A number of radioactive peaks were detected. Based on the mass spectra (Figs. 2 and 3), the main peak, which elutes

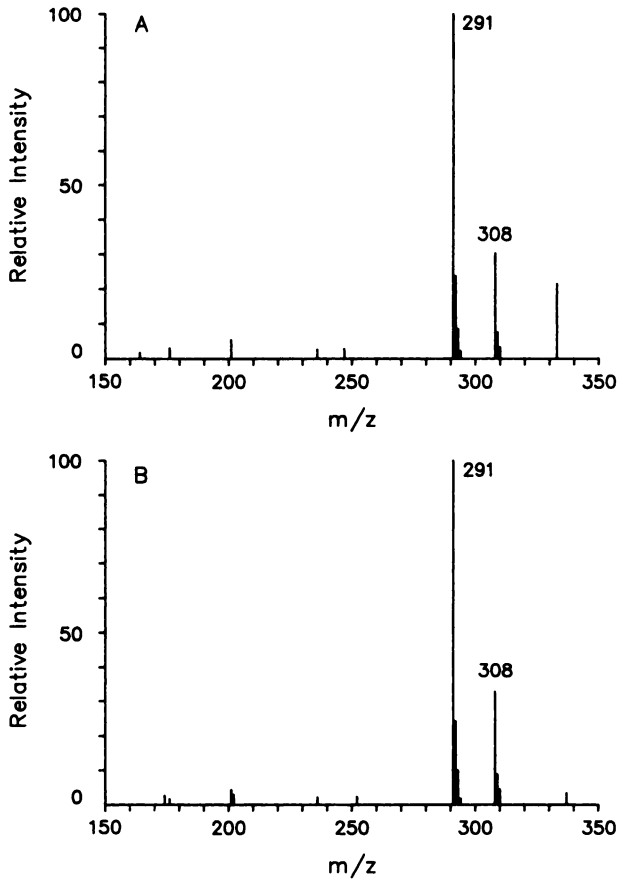

FIGURE 3
Mass spectrum of di-TMS-3-methylglutarate under ammonia chemical ionization. Same standard (A) and rat liver perfusate extract (B) as in Figure 2.

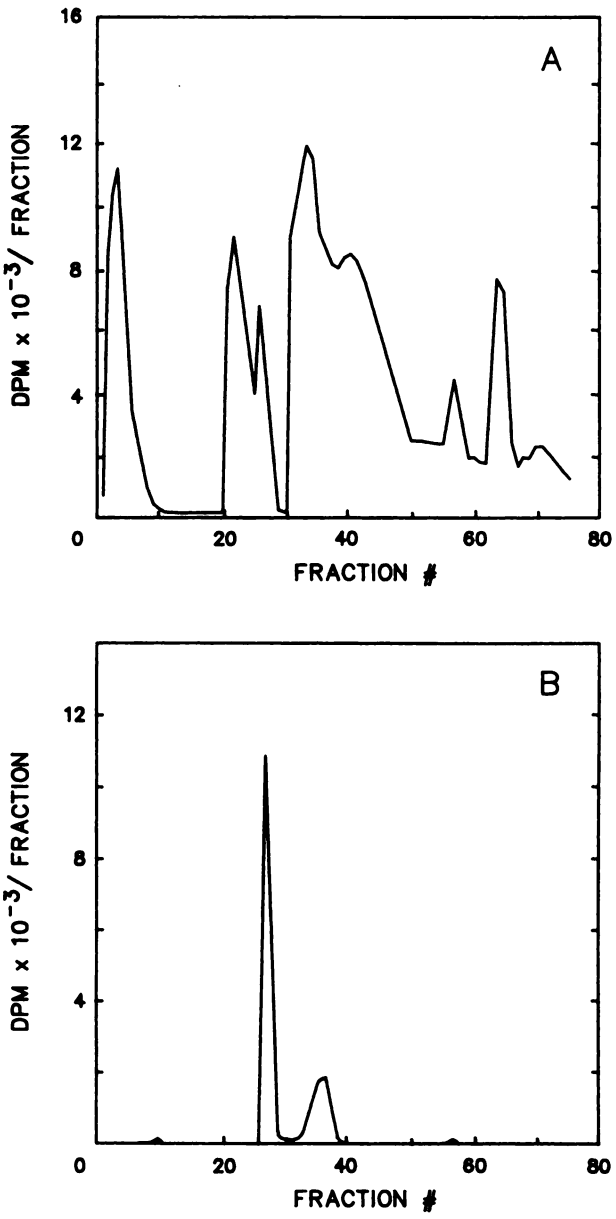

FIGURE 4
Radio-chromatogram of water soluble catabolites of [1-^{14}C] BMHDA and [1-^{14}C]stearate in perfused rat liver. (A) Liver was perfused with 0.75 m*M* of [1-^{14}C]BMHDA. Identification of 3-methyl[1-^{14}C]glutarate in fractions 31 to 43 was obtained by GC-MS analysis. Enzymatic and GC-MS assays identified 3-hydroxybutyrate, lactate, and acetoacetate in fractions 27 to 30, 27 to 34, and 31 to 38, respectively. (B) Liver was perfused with 1 m*M* [1-^{14}C]stearate. The two radioactive peaks were identified by enzymatic and GC-MS assays as R-3-hydroxybutyrate and acetoacetate.

between fractions 31 and 43, appears to be 3-methyl-[1-^{14}C]glutarate. The other peaks could not be identified. In a control experiment, a liver was perfused with 1 m*M* [1-^{14}C]stearate. Chromatography of an extract of the final perfusate shows only two radioactive peaks (Fig. 4B) corresponding to R-3-hydroxybutyrate and acetoacetate (*26*).

DISCUSSION

Production of $^{14}CO_2$ from [1-^{14}C]BMHDA is ascribed to alpha-oxidation which presumably yields unlabeled 2-methyl-hexadecanoate. The latter can undergo beta-oxidation to form 1 propionyl-CoA + 7 acetyl-CoA. In heart and liver, propionyl-CoA is converted to succinyl-CoA, an intermediate of the citric acid cycle. In the liver, propionyl-CoA is a gluconeogenic intermediate. Both heart and liver oxidize acetyl-CoA via the citric acid cycle.

Production of hydrosoluble non-volatile [^{14}C]metabolites from [1-^{14}C]BMHDA is largely due to omega-oxidation, which presumably yields β-methyl-[1-^{14}C] heptadecanedioate. The latter could undergo up to 6 beta-oxidation cycles generating 6 acetyl-CoA + one 3-methyl-[1-^{14}C]glutarate. Incomplete beta-oxidation could yield various 3-methyl-[1-^{14}C]dicarboxylates. Alternatively, β-methyl-[1-^{14}C]heptadecanedioate could conceivably undergo alpha-oxidation to unlabeled 2-methyl-hexadecanedioate. Beta-oxidation of the latter, from the omega end, would yield various 2-methyl-dicarboxylates, down to 2-methyladipate. Beta-oxidation from the alpha end would yield various straight chain dicarboxylates down to adipate.

Chromatography of extracts of final liver perfusate (Fig. 4A) showed the presence of a number of ^{14}C-catabolites of [1-^{14}C]BMHDA. Since 17.6% of the 15 μmole dose of [1-^{14}C]BMHDA was converted to water-soluble ^{14}C-catabolites (Table 3), the maximal concentration of all 3-methyl-dicarboxylates would be 22 nmol/ml and each species would be present at an even lower concentration. Using GC-MS analysis, we could identify 3-methylglutarate only from a 0.75-m*M* BMHDA liver perfusion. The concentration of other acidic metabolites would also be very low and GC-MS analysis could not identify any of the species.

The presence of a methyl group on C-3 of BMHDA blocks beta-oxidation at the level of S-3-hydroxy-acyl-CoA dehydrogenase. Thus, beta-oxidation of S-BMHDA presumably stops at S-3-hydroxy-3-methyl-heptadecanoyl-CoA. R-BMHDA may not undergo dehydrogenation if long-chain acyl-CoA dehydrogenase requires that the hydrogen on C-3 be in the S-configuration. The known mechanism of long-chain acyl-CoA dehydrogenase (*29,30*) does not answer this question. One could wonder whether the 3-methyl-acyl-CoA and/or the 3-hydroxy-3-methyl-acyl-CoA(s) derived from RS-BMHDA could act as a coenzyme A trap. This is not the case since in hearts perfused with 0.1 m*M* BMHDA, there was no accumulation of long-chain acyl-CoA derivatives and no significant decrease in free coenzyme A (Table 2). Therefore, it appears that metabolism of RS-BMHDA does not affect markedly mitochondrial free coenzyme A. Alternatively, the presence of a methyl group on C-3 may prevent transportation of BMHDA to the mitochondria via carnitine acyl transferase, as is the case for β-methyl-15-p-iodophenyl-pentadecanoate (*31*).

Most of the radioactivity of [1-^{14}C]BMHDA is accounted for in heart and liver perfusions (94%–96%, Table 3). Thus, one can calculate the distribution of BMHDA metabolism via alpha-oxidation, omega-oxidation, and esterification to lipids (Table 5). In the heart, 66% of BMHDA is omega-oxidized and 33% is esterified. Alpha-oxidation accounts for less than 1% of BMHDA metabolism in the heart. In the liver by contrast, 53% of BMHDA metabolism occurs via alpha-oxidation. Omega-oxidation and esterification account for 27% and 20% of BMHDA metabolism, respectively.

Since both the liver and the heart actively take up and metabolize FAs, it is unlikely that one could design a labeled MFA that would image the heart specifically. Imaging the liver at the same time as the heart is a minor inconvenience if one can achieve a reasonable residence time of the tracer in the heart. This can be conveniently obtained by blocking beta-oxidation of the MFA. Our data show that BMHDA does not have any detectable deleterious effect on the heart or the liver, when used at doses up to 1000 times that used for myocardial imaging (*32*). Although we have not identified all the catabolites of BMHDA, it is most likely that these anionic compounds are innocuous at the concentrations reached under clinical conditions. One could question whether BMHDA should be used in patients suffering from Refsum's disease, characterized

TABLE 5
Distribution of [1-^{14}C]BMHDA Metabolism in Perfused Liver and Heart

	Heart		Liver	
	μmole/110 min	%	μmole/110 min	%
Alpha-oxidation	0.014 ± 0.02	0.85 ± 0.12	4.60 ± 0.59	52.8 ± 6.8
Omega-oxidation	1.08 ± 0.27	65.9 ± 16.4	2.39 ± 0.41	27.1 ± 4.7
Esterification	0.54 ± 0.11	33.1 ± 6.74	1.76 ± 0.34	20.1 ± 3.9

by a defect in alpha-oxidation (*33*). However, these patients should have normal omega-oxidation and should be able to catabolize the minute diagnostic doses of BMHDA.

ACKNOWLEDGMENTS

This work was supported by grants MA-9771 and DG-395 from the Medical Research Council of Canada (to HB) and grant HL-29636 from the National Institutes of Health, USA (to HWS).

REFERENCES

1. Bailey IK, Griffith LSC, Rouleau J, Strauss HW, Pitt B. Thallium-201 myocardial perfusion imaging at rest and during exercise. Comparative sensitivity to electrocardiography in coronary artery disease. *Circulation* 1977; 55:79–87.
2. Ritchie JL, Zaret BL, Strauss HW, et al. Myocardial imaging with thallium-201: a multicenter study in patients with angina pectoris or acute myocardial infarction. *Am J Cardiol* 1978; 42:345–350.
3. Van der Wall EE, Heidendal GAK, Den Hollander W, Westera G, Roos JP. I-123-labeled hexadecanoic acid in comparison with thallium-201 for myocardial imaging in coronary heart disease. A preliminary study. *Eur J Nucl Med* 1980; 5:401–405.
4. Freundlieb C, Hoeck A, Vyska K, Feinendegen LE, Machulla HJ, Stoecklin G. Myocardial imaging and metabolic studies with [17-I-123]iodoheptadecanoic acid. *J Nucl Med* 1980; 21:1043–1050.
5. Dudczak R, Kletter K, Frischauf H, Losert U, Angelberger P, Schmolinear R. The use of I-123-labeled heptadecanoic acid (HDA) as metabolic tracer: preliminary report. *Eur J Nucl Med* 1984; 9:81–85.
6. Weiss ES, Hoffman EJ, Phelps ME, et al. External detection and visualization of myocardial ischemia with C-11-substrates in vitro and in vivo. *Circ Res* 1976; 39:24–32.
7. Weiss ES, Ahmed SA, Welch MJ, Williamson JR, Ter-Pogossian MM, Sobel BE. Quantification of infarction in cross sections of canine myocardium in vivo with positron emission transaxial tomography and C-11-palmitate. *Circulation* 1977; 55:66–73.
8. Lerch RA, Ambos HD, Bergmann SR, Welsh MJ, Ter-Pogossian MM, Sobel BE. Localization of viable ischemic myocardium by positron-emission tomography with C-11-palmitate. *Circulation* 1981; 64:689–699.
9. Van der Wall EE. Myocardial imaging with radiolabelled free fatty acids: a critical review. *Eur Heart J* 1985; 6:29–38.
10. Livni E, Elmaleh DR, Levy S, Brownell GL, Strauss WH. Beta-methyl[1-^{11}C]heptadecanoic acid: a new myocardial metabolic tracer for positron emission tomography. *J Nucl Med* 1982; 23:169–175.
11. Elmaleh DR, Livni E, Levy S, Varnum D, Strauss HW, Brownell GL. Comparison of ^{11}C and ^{14}C-labeled fatty acids and their β-methyl analogs. *Int J Nucl Med Biol* 1983; 10:181–187.
12. Abendschein DR, Fox KAA, Ambos HD, Sobel BE, Bergmann SR. Metabolism of beta-methyl[1-^{11}C]heptadecanoic acid in canine myocardium. *Nucl Med Biol (Int J Radiat Appl Instrum)* 1987; 14:579–585.
13. Brunengraber H, Boutry M, Lowenstein JM. Fatty acid, 3-β-hydroxysterol, and ketone synthesis in the perfused rat liver. *Eur J Biochem* 1978; 82:373–384.
14. Neely JR, Liebermeister H, Battersby EJ, Morgan HE. Effect of pressure development on oxygen consumption by isolated rat heart. *Am J Physiol* 1967; 212:804–814.
15. Taegtmeyer H, Hems R, Krebs HA. Utilization of energy-providing substrates in the isolated working rat heart. *Biochem J* 1980; 186:701–711.
16. Bünger R, Sommer O, Walter G, Stiegler H, Gerlach E. Functional and metabolic features of an isolated perfused guinea pig heart performing pressure-volume work. *Pflügers Arch* 1979; 380:259–266.
17. Brunengraber H, Boutry M, Lowenstein JM. Fatty acid and 3-β-hydroxysterol synthesis in the perfused rat liver. *J Biol Chem* 1973; 248:2656–2669.
18. Gavino VC, Somma J, Philbert L, David F, Garneau M, Bélair J, Brunengraber H. Production of acetone and conversion of acetone to acetate in the perfused rat liver. *J Biol Chem* 1987; 262:6735–6740.
19. Bergmeyer HU, Bernt E, Schmidt F, Stork H. D-Glucose. Determination with hexokinase and glucose-6-phosphate dehydrogenase. In: Bergmeyer HU, ed. *Methods of enzymatic analysis, Vol. 3.* New York: Academic Press; 1974:1196–1201.
20. Gutmann I, Wahlefeld AG. L-(+)-Lactate. Determination with lactate dehydrogenase and NAD. In: Bergmeyer HU, ed. *Methods of enzymatic analysis, Vol. 3.* New York: Academic Press; 1974:1464–1468.
21. Folch J, Lees M, Sloane Stanley GH. A simple method for the isolation and purification of total lipids from animal tissues. *J Biol Chem* 1957; 226:497–509.
22. Williamson JR, Corkey BE. Assays of intermediates of citric acid cycle and related compounds by fluorometric enzyme methods. *Methods Enzymol* 1969; 13:434–513.
23. Lamprech W, Trautschold I. Adenosine-5′-triphosphate. Determination with hexokinase and glucose-6-phosphate dehydrogenase. In: Bergmeyer HU, ed. *Methods of enzymatic analysis, Vol. 4.* New York: Academic Press; 1974:2101–2110.
24. Keppler D. Determination of 5′-nucleotides as nucleoside-5′-monophosphates. In: Bergmeyer HU, ed. *Methods of enzymatic analysis, Vol. 4.* New York: Academic Press; 1974:2088–2096.
25. Lamprech W, Stein P, Heinz F, Weisser H. Creatine phosphate. Determination with creatine kinase, hexokinase, and glucose-6-phosphate dehydrogenase. In: Bergmeyer HU, eds. *Methods of enzymatic analysis, Vol. 4.* New York: Academic Press; 1974:1777–1785.
26. Endemann G, Goetz PG, Edmond J, Brunengraber H. Lipogenesis from ketone bodies in the isolated perfused rat liver. *J Biol Chem* 1982; 257:3434–3440.
27. Des Rosiers C, Montgomery JA, Desrochers S, et al. Interference of 3-hydroxyisobutyrate with measurements of ketone body concentration and isotopic enrichment by gas chromatography-mass spectrometry. *Anal Biochem* 1988; 173:96–105.
28. Scholz R, Schwabe U, Soboll S. Influence of fatty acids on energy metabolism. 1. Stimulation of oxygen consumption, ketogenesis and CO_2 production following addition of octanoate and oleate in perfused rat liver. *Eur J Biochem* 1984; 141:223–230.
29. Bielmann JF, Hirth CG. Stereochemistry of the oxidation at the α-carbon of butyryl-CoA and of the enzymic hydrogen exchange. *FEBS* 1970; 9:335–336.
30. Ikeda Y, Hine DG, Okamura-Ikeda K, Tanaka K. Mechanism of action of short-chain, medium-chain, and long-chain acyl-CoA dehydrogenases. *J Biol Chem* 1985; 260:1326–1337.

31. DeGrado TR, Holden JE, Ng CK, Raffel DM, Gatley SJ. β-Methyl-15-p-iodophenylpentadecanoic acid metabolism and kinetics in the isolated rat heart. *Eur J Nucl Med* 1989; 15:78–80.
32. Elmaleh DR, Livni E, Levy S, Varnum D, Strauss HW, Brownell GL. Comparison of C-11- and C-14-labeled fatty acids and their beta methyl analogs. *Int J Nucl Med* 1983; 10:181–187.
33. Eldjarn L, Try K, Stokke O. The existence of an alternative pathway for the degradation of branch-chained fatty acids, and its failure in heredopathia atactica polyneuritiformis (Refsum's disease). *Biochim Biophys Acta* 1966; 116:395–397.

SELF-STUDY TEST

Skeletal Nuclear Medicine

Questions are taken from the *Nuclear Medicine Self-Study Program I*, published by The Society of Nuclear Medicine

DIRECTIONS

The following items consist of a heading followed by lettered options related to that heading. Select the options that you think are true and those that you think are false. Answers may be found on page 1838.

1. A 55-year-old woman consulted her physician because of back pain. Antero-posterior and lateral radiographs of the lumbar spine and chest revealed a vertebral body compression fracture at T10 and wedging of the L1 body. True statements concerning this patient include which of the following?

A. Osteoporosis is the most likely diagnosis.
B. The age of the compression fracture likely can be determined from the spinal radiographs.
C. Further evaluation should include both bone mineral measurements and iliac crest biopsy.
D. Based on the radiographic findings, treatment with estrogen should be started.

2. True statements regarding bone mineral measurements include which of the following?

A. Axial skeletal sites generally are preferable to peripheral skeletal sites for clinical measurements of bone mineral in patients with suspected osteoporosis.
B. They reliably distinguish osteomalacia from osteoporosis.
C. They are helpful for determining fracture risk at a specific skeletal site.
D. The importance of bone mineral as a predictor of fracture varies between skeletal sites.
E. The "fracture threshold" is that bone mineral level below which bone fracture always occurs.

3. True statements concerning the treatment of osteoporosis include which of the following?

A. Calcitonin and calcium (1500 mg/day orally) will substantially increase the patient's bone mass.
B. Dietary supplementation with calcium alone is inferior to combination therapy with estrogen and calcium in the treatment of postmenopausal osteoporosis.
C. Fluoride has proven to be an ineffective form of therapy.
D. The effect of estrogen on bone mass can be measured equally well in the lumbar spine or in the radius.
E. A follow-up bone mineral measurement 3 months after instituting treatment usually is sufficient to monitor the effectiveness of the treatment.

(continued on page 1838)